

## Highly Potent Half-sandwich Iridium and Ruthenium Complexes as Lysosome-Targeted Imaging and Anticancer agents

JuanJuan Li,<sup>a</sup> Zhenzhen Tian,<sup>a</sup> Zhishan Xu,<sup>a, b</sup> Shumiao Zhang,<sup>a</sup> Yaqian Feng,<sup>a</sup> Lingdong Zhang,<sup>a</sup> Zhe Liu<sup>a\*</sup>

<sup>a</sup> Institute of Anticancer Agents Development and Theranostic Application, The Key Laboratory of Life-Organic Analysis and Key Laboratory of Pharmaceutical Intermediates and Analysis of Natural Medicine, Department of Chemistry and Chemical Engineering, Qufu Normal University, Qufu 273165, China.

<sup>b</sup> Department of Chemistry and Chemical Engineering, Shandong Normal University, Jinan 250014, China.

\*Corresponding author. Email: [liuzheqd@163.com](mailto:liuzheqd@163.com)

### Supporting Information

EXPERIMENTAL SECTION .....	2
Fig. S1 – Fig. S8.....	6
Table S1 – Table S14 .....	13
Fig. S9 – Fig. S20.....	26
References .....	32

## Experimental Section

**Materials and Instrumentation.** Unless otherwise noted, all manipulations were performed using standard Schlenk tube techniques under nitrogen atmosphere. The reagents  $\text{IrCl}_3 \cdot n\text{H}_2\text{O}$  ( $\geq 99\%$  purity), hydrated  $\text{RuCl}_3 \cdot n\text{H}_2\text{O}$  ( $\geq 99\%$  purity), octan-1-ol ( $\geq 99\%$ ), and Nitric acid (72%), 2,3,4,5-tetramethyl-2-cyclopentenone (95%), 1,2,3,4,5-pentamethyl-cyclopentadiene (95%), butyllithium solution (1.6 M in hexane), 1,2-bis(diphenylphosphino)benzene(98%), 1,8-bis(diphenylphosphino)naphthalene(98%), 4-phenylbutan-1-ol were purchased from Sigma-Aldrich.  $\text{Cp}^{\text{xbiph}}\text{H}^1$  and  $[(\eta^6\text{-bz-BA})\text{RuCl}_2]_2$  (**dimer3**)<sup>2</sup> were prepared as described. For the biological experiments, Hoechst 33342(apoptosis and epigenetic company), 3-methyladenine (apoptosis and epigenetic company), cycloheximide, leupeptin, necrostatin-1, carbonyl cyanide m-chlorophenylhydrazone (CCCP), Z-VAD-FMK and cleaved Caspase-3 were purchased from apoptosis and epigenetic company, MTDR (Life Technologies), LTDR (Life Technologies), MTT (3-(4,5-dimethylthiazol-2-yl)-2,5-diphenyltetrazolium bromide, Sigma-Aldrich), Annexin V-FITC Apoptosis Detection Kit (Sigma-Aldrich), JC-1 (Sigma-Aldrich), PBS (Sangon Biotech), PI (Sigma-Aldrich) are all used as received. Supercoiled pBR322 DNA and 6X loading buffer (0.05% bromophenol blue, 0.035% xylene cyanol FF, 36% glycerol and 30 mM EDTA were purchased from TaKaRa Biotechnology (Dalian, China). DMEM medium, fetal bovine serum, penicillin/streptomycin mixture, trypsin/EDTA, and phosphate-buffered saline (PBS) were purchased from Sangon Biotech. Testing compounds was dissolved in DMSO and diluted with the tissue culture medium before use.

**X-ray Crystallography.** All diffraction data were obtained on a Bruker Smart Apex CCD diffractometer equipped with graphite-monochromated Mo  $K\alpha$  radiation. Absorption corrections were applied using SADABS program. The crystals were mounted in oil and held at 100 K with the Oxford Cryosystem Cobra. The structures were solved by direct methods using SHELXS (TREF) with additional light atoms found by Fourier methods. Complexes were refined against F<sub>2</sub> using SHELXL, and hydrogen atoms were added at calculated positions and refined riding on their parent atoms. X-ray crystallographic data for complexes **Ir1** and **Ir4** are available as **Figure 1**, **Tables 1-2** and have been deposited in the Cambridge Crystallographic Data Centre under the accession numbers 1841367 (**Ir1**) and 1841368 (**Ir4**), respectively. X-ray crystallographic data in CIF format are available from the Cambridge Crystallographic Data Centre.

**NMR Spectroscopy.** <sup>1</sup>H NMR spectra were acquired in 5 mm NMR tubes at 298 K on Bruker DPX 500 (<sup>1</sup>H = 500.13 MHz) spectrometers. <sup>1</sup>H NMR chemical shifts were internally referenced to  $(\text{CHD}_2)(\text{CD}_3)\text{SO}$  (2.50 ppm) for  $\text{DMSO-}d_6$ ,  $\text{CDCl}_3$  (7.26 ppm) (for chloroform- $d_1$ ), MeOD(3.31 ppm), All data processing was carried out using XWIN-NMR version 3.6 (Bruker UK Ltd.).

**UV-Vis Spectroscopy.** A TU-1901 UV-Vis recording spectrophotometer was used with 1 cm path-length quartz cuvettes (3 mL). Spectra were processed using UVWinlab software. Experiments were carried out at 298 K unless otherwise stated.

**Fluorescence measurements.** A F-4600 fluorescence spectrophotometer was used with 1 cm path-length quartz cuvettes (3ml). Experiments were carried out at room temperature unless otherwise stated. Experiments were carried out in methanol solutions. Fluorescence spectra were obtained by recording the emission spectra at  $\lambda_{\text{ex}} = 300 \text{ nm}$  (Ex Slit: 10.0 nm, Em Slit: 10.0 nm, PMT Voltage: 500 V).

**Interactions with Nucleobases.** The reaction of complex **Ir3** (ca. 1 mM) with nucleobases typically involved addition of a solution containing 3 mol equiv of nucleobase in D<sub>2</sub>O to an equilibrium solution of complex **Ir3** in 50%

MeOD /50% D<sub>2</sub>O (v/v). <sup>1</sup>H NMR spectra of these solutions were recorded at 310 K after various time intervals.

**Reaction with NADH.** The reaction of complex (ca. 1 μM) with NADH (132 μM) in 50% MeOH/50% H<sub>2</sub>O (v/v) was monitored by UV-Vis at 298 K after various time intervals. TON was calculated from the difference in NADH concentration after 9 h divided by the concentration of iridium catalyst. The concentration of NADH was obtained using the extinction coefficient  $\epsilon_{339} = 6220 \text{ M}^{-1}\text{cm}^{-1}$ .

**Cell Culture.** A549 cervical carcinoma cells were obtained from Shanghai Institute of Biochemistry and Cell Biology (SIBCB) and were grown in Dubelco's Modified Eagle Medium (DMEM). All media were supplemented with 10% fetal bovine serum, and 1% penicillin-streptomycin solution. All cells were grown at 310 K in a humidified incubator under a 5% CO<sub>2</sub> atmosphere.

**Viability assay (MTT assay).** After plating 5000 A549 cells per well in 96-well plates, the cells were preincubated in drug-free media at 310 K for 24 h before adding different concentrations of the compounds to be tested. In order to prepare the stock solution of the drug, the solid complex was dissolved in DMSO. This stock was further diluted using cell culture medium until working concentrations were achieved. The drug exposure period was 24 h. Subsequently, 15 μL of 5 mg mL<sup>-1</sup> MTT solution was added to form a purple formazan. Afterwards, 100 μL of dimethyl sulfoxide (DMSO) was transferred into each well to dissolve the purple formazan, and results were measured using a microplate reader (DNM-9606, Perlong Medical, Beijing, China) at an absorbance of 570 nm. Each well was triplicated and each experiment repeated at least three times. IC<sub>50</sub> values quoted are mean ± SEM.

**Localization Experiments.** Localization of complex **Ir3** (10 μM) with mitochondria or lysosome were examined by means of MTDR (MitoTracker Deep Red) (Molecular Probes), a mitochondria-specific dye and LTDR (LysoTracker Deep Red), a lysosome-specific dye. Briefly, A549 cells were seeded into 6-well plates (Greiner, Germany) for confocal microscopy. After cultured overnight, a 1 mM **Ir3** stock solution made in DMSO was diluted to 10 μM working concentration in cell medium (DMEM, 5% FCS). Staining of mitochondria/lysosome was accomplished by adding a 75 nM/100 nM final concentration of MTDR/LTDR to the culture medium for the last 30 min of complex incubation. The medium was removed and washed three times with ice-cold PBS, and then viewed immediately under a confocal microscope (Zeiss LSM880 NLO). The excitation and emission bands of each compound were selected as follows for **Ir3**:  $\lambda_{\text{ex}} = 488 \text{ nm}$ ,  $\lambda_{\text{em}} = 520 \pm 30 \text{ nm}$ ; MTDR:  $\lambda_{\text{ex}} = 644 \text{ nm}$ ,  $\lambda_{\text{em}} = 700 \pm 30 \text{ nm}$ ; for LTDR:  $\lambda_{\text{ex}} = 594 \text{ nm}$ ,  $\lambda_{\text{em}} = 630 \pm 30 \text{ nm}$ .

**Cellular Uptake.** A549 cells were seeded in 6-well plates for 24 h and preincubated with CCCP (50 μM) or chloroquine (50 μM) for 1 h. The medium was removed and the cells were then incubated with **Ir3** (10 μM) for 1 h. To investigate the impact of temperature on cellular uptake, the cells were incubated at 4 °C or 37 °C for 1 h. In each case, the cells were washed three times with ice-cold PBS and visualize by confocal microscopy (Zeiss LSM880NLO) immediately.  $\lambda_{\text{ex}} = 488 \text{ nm}$ ,  $\lambda_{\text{em}} = 520 \pm 30 \text{ nm}$ .

**AO staining.** A549 cells seeded into 35 mm dishes (Corning) were exposed to complex **Ir3** at the indicated concentrations for 1 h and 12 h, cells were then washed twice with PBS and incubated with AO (5 μM) at 37 °C for 15 min. The cells were washed twice with PBS and visualized by confocal microscopy (Zeiss LSM880NLO). Emission was collected at  $510 \pm 20 \text{ nm}$  (green) and  $625 \pm 20 \text{ nm}$  (red) upon excitation at 488 nm.

**Detection of cathepsin B release.** Cathepsin B activity was detected using the fluorogenic substrate Magic Red MR-(RR)<sub>2</sub> according to the manufacturer's instructions. Briefly, A549 cells seeded into 35 mm dishes (Corning) were exposed to complex Ir3 at the indicated concentrations for 12 h. The media was removed and the cells were washed twice with PBS and then incubated with cathepsin B substrate at 37 °C for 1 h. The media was removed and the cells were washed twice with PBS and visualized by confocal microscopy (Zeiss LSM880NLO).  $\lambda_{\text{ex}} = 543 \text{ nm}$ ,  $\lambda_{\text{em}} = 630 \pm 20 \text{ nm}$ .

**Caspase-3 activity assay.** Flow cytometry analysis of Caspase-3 activity in A549 cells caused by exposure to metal complexes was carried out using the Caspase-Glo® Assay kit according to the manufacturer's instructions. Briefly, cells were cultured in six-well plate and preincubated in drug-free media at 310 K for 24 h. After A549 cells were incubated with Ir3 for 24 h at concentrations of  $0.5 \times \text{IC}_{50}$ ,  $\text{IC}_{50}$ ,  $2 \times \text{IC}_{50}$  and  $3 \times \text{IC}_{50}$ , 10  $\mu\text{L}$  of Caspase-Glo®3 reagent was added to each well containing 2000  $\mu\text{L}$  culture media. The mixture was incubated at room temperature for 1 h and then washed triple immediately with PBS. The fluorescence intensity was analyzed by flow cytometry (ACEA NovoCyte, Hangzhou, China). Data were processed using NovoExpress™ software.

**Z-VAD-fmk activity assay.** A549 cells at  $1.5 \times 10^6$  per well were seeded in a six-well plate. Cells were preincubated in drug-free media at 310 K for 24 h, after which drugs were added at concentrations of  $0.5 \times \text{IC}_{50}$ ,  $\text{IC}_{50}$ ,  $2 \times \text{IC}_{50}$  and  $3 \times \text{IC}_{50}$ . Caspases inhibitor z-VAD-fmk (5  $\mu\text{M}$ ) was added 30 min earlier before cells were treated with drugs. After 24 h of drug exposure, cells were collected, washed once with PBS, and resuspended in 195  $\mu\text{L}$  of annexin V-FITC binding buffer which was then added to 5  $\mu\text{L}$  of annexin V-FITC and 10  $\mu\text{L}$  of PI, and then incubated at room temperature in the dark for 15 min. Subsequently, the buffer placed in an ice bath in the dark. The samples were analyzed by a flow cytometer (ACEA NovoCyte, Hangzhou, China).

**Induction of Apoptosis.** Flow cytometry analysis of apoptotic populations of A549 cells caused by exposure to metal complexes was carried out using the Annexin V-FITC Apoptosis Detection Kit (Beyotime Institute of Biotechnology, China) according to the supplier's instructions. Briefly, A549 cells ( $1.5 \times 10^6$  /2 mL per well) were seeded in a six-well plate. Cells were preincubated in drug-free media at 310 K for 24 h, after which drugs were added at concentrations of  $0.5 \times \text{IC}_{50}$ ,  $1 \times \text{IC}_{50}$ ,  $2 \times \text{IC}_{50}$  and  $3 \times \text{IC}_{50}$ . After 24 h of drug exposure, cells were collected, washed once with PBS, and resuspended in 195  $\mu\text{L}$  of annexin V-FITC binding buffer which was then added to 5  $\mu\text{L}$  of annexin V-FITC and 10  $\mu\text{L}$  of PI, and then incubated at room temperature in the dark for 15 min. Subsequently, the buffer placed in an ice bath in the dark. The samples were analyzed by a flow cytometer (ACEA NovoCyte, Hangzhou, China).

**Cell Cycle Analysis.** A549 cells at  $1.5 \times 10^6$  per well were seeded in a six-well plate. Cells were preincubated in drug-free media at 310 K for 24 h, after which drugs were added at concentrations of  $0.25 \times \text{IC}_{50}$ ,  $0.5 \times \text{IC}_{50}$  and  $\text{IC}_{50}$ . After 24 h or 48 h of drug exposure, supernatants were removed by suction and cells were washed with PBS. Finally, cells were harvested using trypsin-EDTA and fixed for 24 h using cold 70 % ethanol. DNA staining was achieved by resuspending the cell pellets in PBS containing propidium iodide (PI) and RNase. Cell pellets were washed and resuspended in PBS before being analyzed in a flow cytometer (ACEA NovoCyte, Hangzhou, China) using excitation of DNA-bound PI at 488 nm, with emission at 585 nm. Data were processed using NovoExpress™ software. The cell cycle distribution is shown as the percentage of cells containing G<sub>0</sub>/G<sub>1</sub>, S G<sub>2</sub>/M and Sub-G<sub>1</sub> phase DNA as identified by propidium iodide staining.

**ROS Determination.** Flow cytometry analysis of ROS generation in A549 cells caused by exposure to metal

complexes was carried out using the Reactive Oxygen Species Assay Kit (Beyotime Institute of Biotechnology, Shanghai, China) according to the supplier's instructions. Briefly,  $1.5 \times 10^6$  A549 cells per well were seeded in a six-well plate. Cells were preincubated in drug-free media at 310 K for 24 h or 48 h in a 5% CO<sub>2</sub> humidified atmosphere, and then drugs were added at concentrations of  $0.25 \times IC_{50}$ . After 24 h or 48 h of drug exposure, cells were washed twice with PBS and then incubated with the DCFH-DA probe (10  $\mu$ M) at 37 °C for 30 min, and then washed triple immediately with PBS. The fluorescence intensity was analyzed by flow cytometry (ACEA NovoCyte, Hangzhou, China). Data were processed using NovoExpress™ software. At all times, samples were kept under dark conditions to avoid light-induced ROS production.

**Mitochondrial Membrane Assay.** Analysis of the changes of mitochondrial potential in cells after exposure to iridium complex was carried out using the mitochondrial membrane potential assay kit with JC-1 (Beyotime Institute of Biotechnology, Shanghai, China) according to the manufacturer's instructions. Briefly,  $1.5 \times 10^6$  A549 cancer cells were seeded in six-well plates left to incubate for 24 h or 48 h in drug-free medium at 310 K in a humidified atmosphere. Drug solutions, at concentrations of  $0.25 \times IC_{50}$ ,  $0.5 \times IC_{50}$ ,  $1 \times IC_{50}$  and  $2 \times IC_{50}$  of drug against A549 cancer cells, were added in triplicate, and the cells were left to incubate for a further 24 h under similar conditions. Supernatants were removed by suction, and each well was washed with PBS before detaching the cells using trypsin-EDTA. Staining of the samples was done in flow cytometry tubes protected from light, incubating for 30 min at ambient temperature. The samples were immediately analyzed by a flow cytometer (ACEA NovoCyte, Hangzhou, China). For positive controls, the cells were exposed to carbonyl cyanide 3-chlorophenylhydrazone, CCCP (5  $\mu$ M), for 20 min. Data were processed using NovoExpress™ software.

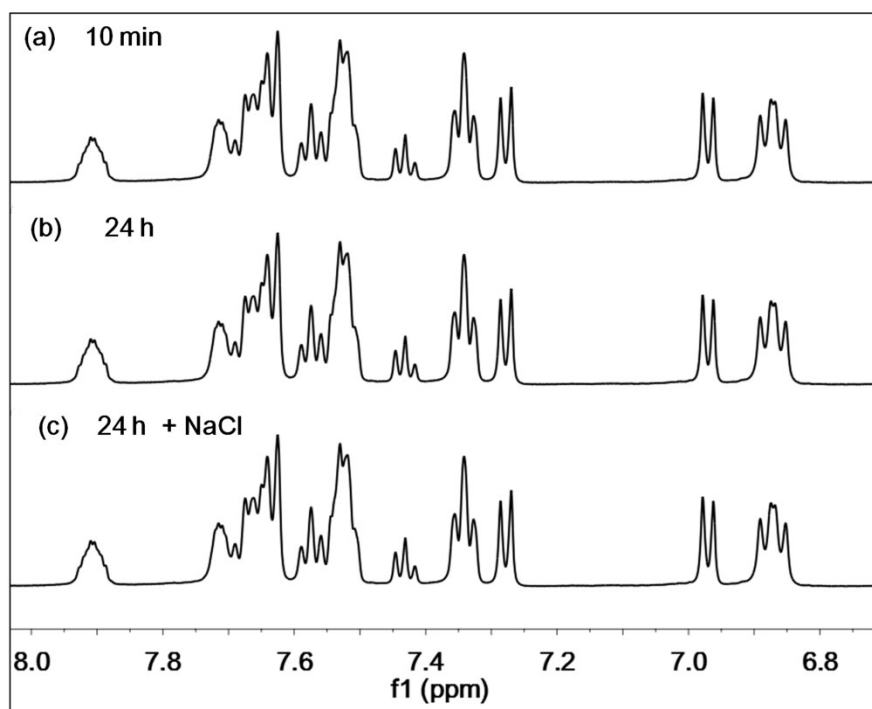


Fig. S1.  $^1\text{H}$  NMR spectra showed no hydrolysis for complex **Ir3** (1 mM) in 50% MeOD /50%  $\text{D}_2\text{O}$  (v/v) at 310 K. (a) after 10 min; (b) after 24 h ; (c) 2 h after addition of 16 mol equiv of NaCl.

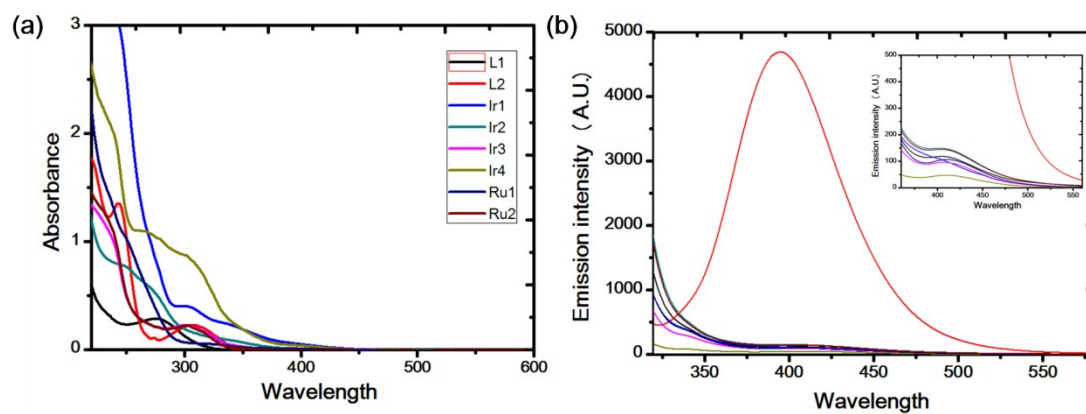


Fig. S2. (a) UV-Vis spectrum and (b) emission spectra ( $\lambda_{\text{ex}} = 300 \text{ nm}$ ) for 20  $\mu\text{M}$  solution of ligands **L1**, **L2** and complexes **Ir1-Ir4**, **Ru1-Ru2**, in methanol solutions.

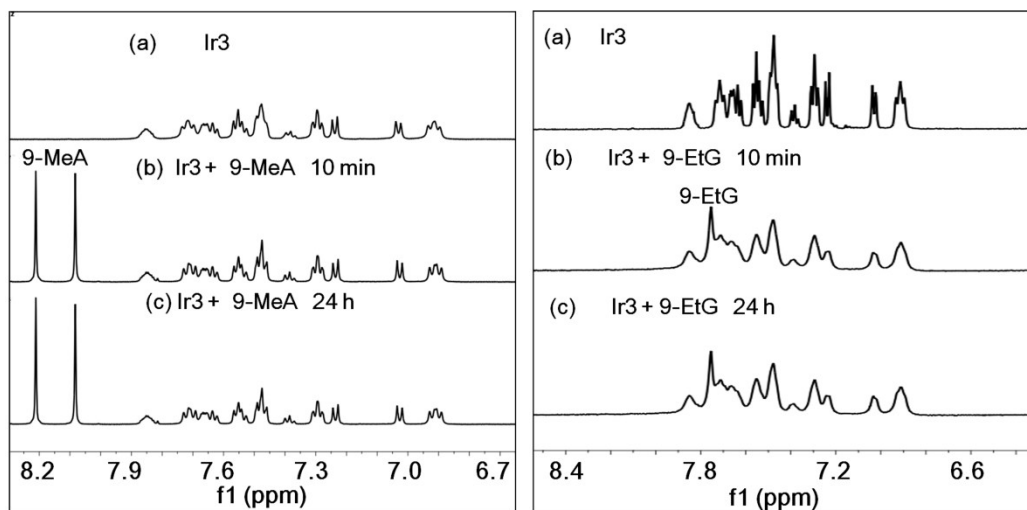


Fig. S3. Low-field region of the  $^1\text{H}$  NMR spectra for reaction of **Ir3** with 9-MeA or 9-EtG. (a)  $^1\text{H}$  NMR spectra for complex **Ir3** (1 mM) in 50% MeOD /50%  $\text{D}_2\text{O}$  (v/v) after 24 h; (b) 10 min after addition of 3 mol equiv of 9-MeA or 9-EtG to solution of complex **Ir3** (1.0 mM); (c) after 24h.

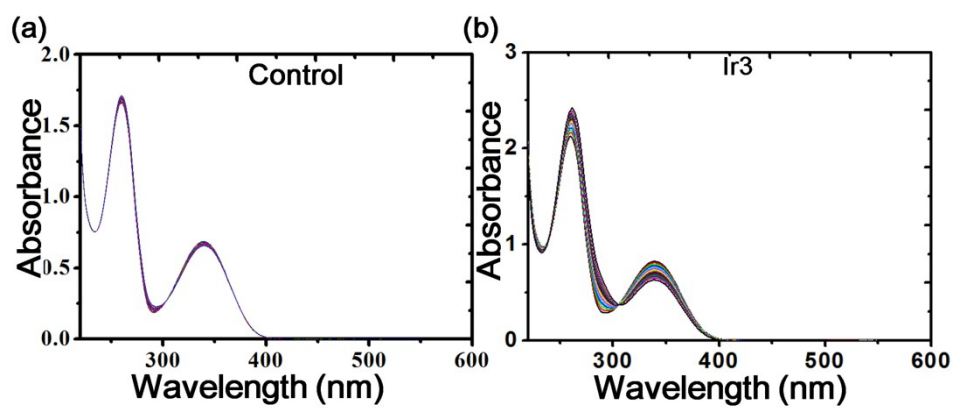


Fig. S4. (a) UV-Vis spectra of the reaction of NADH (100  $\mu\text{M}$ ) in 50% MeOH /50% H<sub>2</sub>O (v/v) at 298 K for 9 h. (b) UV/Vis spectra of the reaction of NADH (132  $\mu\text{M}$ ) with (Ir3) (1  $\mu\text{M}$ ).

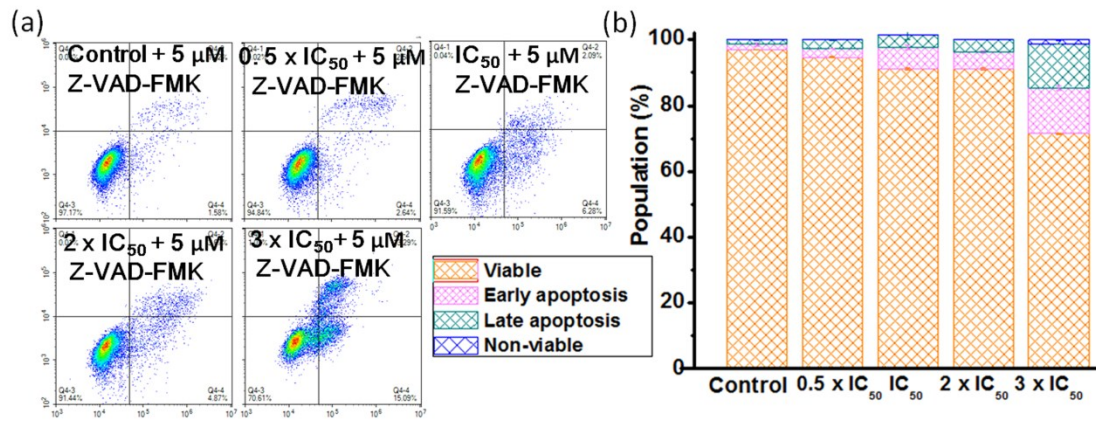


Fig. S5. Flow cytometry detected the apoptosis based on Annexin V/PI assay of A549 cells treated with complex **Ir3**, and the pan-caspase inhibitor Z-VAD-FMK for 24 h at 310 K. (a) Populations for cells treated with different concentrations of **Ir3** and Z-VAD-FMK (5 μM); (b) Histogram for A549 cells treated by **Ir3** and Z-VAD-FMK (5 μM) for 24 h.

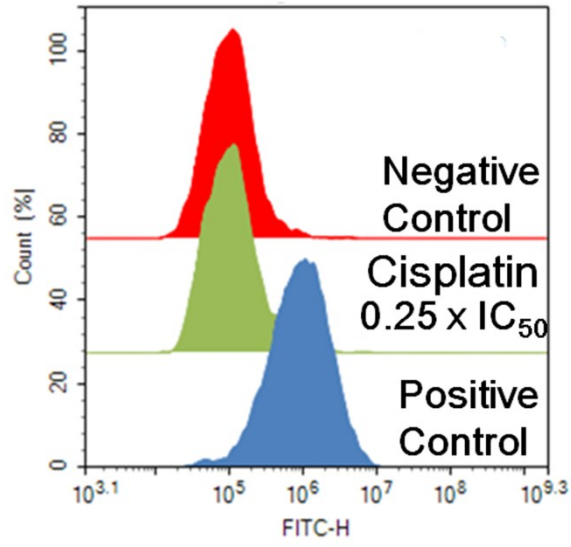


Fig. S6. Flow cytometry analysis on ROS induction after 48 h in A549 cancer cells treated with cisplatin at concentrations of  $0.25 \times IC_{50}$ .

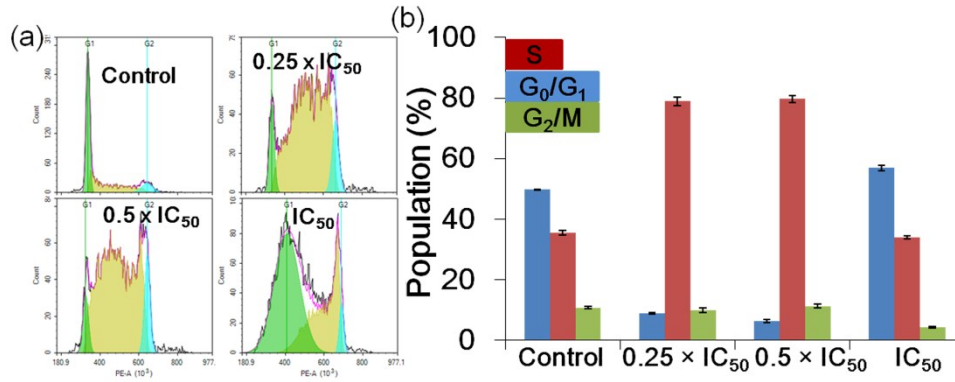


Fig. S7. Cell cycle analysis of A549 cancer cells after 48 h of exposure to cisplatin at 310 K. Concentrations used were 0.25, 0.5 and 1 equipotent concentrations of IC<sub>50</sub>. Cell staining for flow cytometry was carried out using PI. (a) Cell populations in each cell cycle phase for control and cisplatin at various concentrations. (b) Histogram for negative control (cells untreated) and cisplatin.

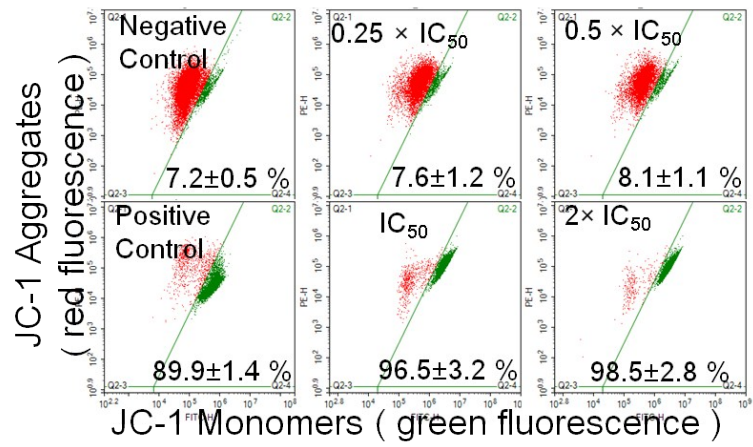


Fig. S8. Effects of cisplatin on MMP analyzed by JC-1 staining and flow cytometry. A549 cells were treated with vehicle or cisplatin at the indicated concentrations for 48 h.

Table S1. Crystallographic Data for  $[(\eta^5\text{-Cp}^*)\text{Ir}(\text{L1})\text{Cl}]\text{PF}_6$  (**Ir1**), and  $[(\eta^5\text{-Cp}^{\text{xbiph}})\text{Ir}(\text{L2})\text{Cl}]\text{PF}_6$  (**Ir4**).

	<b>Ir1</b>	<b>Ir4</b>
formula	$\text{C}_{41}\text{H}_{43}\text{ClF}_6\text{IrOP}_3$	$\text{C}_{55}\text{H}_{47}\text{ClF}_6\text{IrP}_3$
MW	986.31	1142.49
Cryst size(mm)	0.38 x 0.20 x 0.18	0.42 x 0.32 x 0.04
$\lambda$ (Å)	0.71073	0.71073
temp(K)	295(2)	295(2)
cryst syst	Orthorhombic	Monoclinic
space group	Pbca	P21/C
a (Å)	19.6096(11)	16.0389(9)
b (Å)	17.4627(10)	15.8195(9)
c (Å)	23.4976(13)	19.3415(11)
$\alpha$ (°)	90	90
$\beta$ (°)	90	106.8390(10)
$\gamma$ (°)	90	90
vol(Å <sup>3</sup> )	8046.4(8)	4697.0(5)
Z	8	4
R1[ $I > 2\sigma(I)$ ]	0.0480	0.0254
wR2[ $I > 2\sigma(I)$ ]	0.1100	0.0611
GOF	1.141	1.037

Table S2. Selected Bond Lengths (Å) and Angles (deg) for  $[(\eta^5\text{-Cp}^*)\text{Ir}(\text{L1})\text{Cl}]\text{PF}_6$  (**Ir1**), and  $[(\eta^5\text{-Cp}^{\text{xbiph}})\text{Ir}(\text{L2})\text{Cl}]\text{PF}_6$  (**Ir4**).

	<b>Ir1</b>	<b>Ir4</b>
Ir –C (cyclopentadienyl)	2.209(7)	2.228(3)
	2.228(7)	2.254(3)
	2.225(7)	2.277(3)
	2.250(7)	2.283(3)
	2.256(7)	2.287(3)
Ir –C(centroid)	1.8614	1.9095
Ir –P <sub>1</sub>	2.2967(16)	2.2890(8)
Ir –P <sub>2</sub>	2.2892(17)	2.2986(8)
Ir –Cl	2.3962(17)	2.4023(8)
P <sub>1</sub> – Ir –P <sub>2</sub>	84.27(6)	83.54(3)
P <sub>1</sub> – Ir –Cl	86.01(6)	89.38(3)
P <sub>2</sub> – Ir –Cl	83.65(6)	85.94(3)

Table S3. Photophysical Characteristics of ligands L1, L2 and complexes **Ir1-Ir4**, **Ru1-Ru2**.

Complex	absorption <sup>a</sup> $\lambda$ (nm) ( $\epsilon$ ( $\times 10^4$ M <sup>-1</sup> cm <sup>-1</sup> ))	
<b>L1</b>	275 (1.44)	
<b>L2</b>	243 (6.76)	308 (1.14)
<b>Ir1</b>	306 (1.95)	343 (1.09)
<b>Ir2</b>	249 (3.86)	
<b>Ir3</b>	301(1.14)	
<b>Ir4</b>	268 (5.44)	301 (4.36)
<b>Ru1</b>		
<b>Ru2</b>	302 (1.13)	

<sup>a</sup> In MeOH solutions (20  $\mu$ M).  $\epsilon$  denotes the molar extinction coefficients.

Table S4. Inhibition of Growth of A549 Cancer Cells by Complexes **Ir1-Ir4**, **Ru1-Ru2** and Comparison with Cisplatin Recorded over a Period of 48 h.

Complex	IC <sub>50</sub> ( $\mu$ M)
	A549
$[(\eta^5\text{-Cp}^*)\text{Ir}(\text{L1})\text{Cl}]\text{PF}_6$ ( <b>Ir1</b> )	2.02 $\pm$ 0.14
$[(\eta^5\text{-Cp}^*)\text{Ir}(\text{L2})\text{Cl}]\text{PF}_6$ ( <b>Ir2</b> )	3.04 $\pm$ 0.11
$[(\eta^5\text{-Cp}^{\text{biph}})\text{Ir}(\text{L1})\text{Cl}]\text{PF}_6$ ( <b>Ir3</b> )	0.23 $\pm$ 0.02
$[(\eta^5\text{-Cp}^{\text{biph}})\text{Ir}(\text{L2})\text{Cl}]\text{PF}_6$ ( <b>Ir4</b> )	1.01 $\pm$ 0.02
$[(\eta^6\text{-bz-BA})\text{Ru}(\text{L1})\text{Cl}]\text{PF}_6$ ( <b>Ru1</b> )	0.51 $\pm$ 0.10
$[(\eta^6\text{-bz-BA})\text{Ru}(\text{L2})\text{Cl}]\text{PF}_6$ ( <b>Ru2</b> )	1.32 $\pm$ 0.40
Cisplatin	16.70 $\pm$ 1.40

Table S5. Flow cytometry analysis to determine the percentages of apoptotic cells, using Annexin V-FITC vs PI staining, after exposing A549 cells to complex **Ir3**.

Complex	Ir concentration	Viable	Population (%)		
			Early apoptosis	Late apoptosis	Non-viable
<b>Ir3</b>	0.5 × IC <sub>50</sub>	68.2±3.9	9.4±1.9	19.7±1.7	2.7± 0.3
	1 × IC <sub>50</sub>	60.1±3.3	10.3±2.8	24.6±1.4	5.0±1.3
	2 × IC <sub>50</sub>	60.0±2.5	9.4±0.7	27.8±2.2	3.0±0.6
	3 × IC <sub>50</sub>	43.2±3.4	6.6±0.5	44.0±2.7	6.3±1.2
<b>Control</b>		90.4±0.4	3.4±0.8	6.0±1.2	0.2±0.1

Table S6. Detection of caspase 3 activity in A549 cells after the cells were treated with different concentrations of Ir3.

Complex		Cells in highly Caspase-3 active levels
<b>Ir3</b>	0.5 × IC <sub>50</sub>	2.62±0.03
	1 × IC <sub>50</sub>	6.80±0.05
	2 × IC <sub>50</sub>	15.61±0.12
	3 × IC <sub>50</sub>	42.54±0.31
<b>control</b>		0.92±0.01

Table S7. Flow cytometry analysis to determine the percentages of apoptotic cells, using Annexin V-FITC vs PI staining, after exposing A549 cells to complex **Ir3** and the pan-caspase inhibitor Z-VAD-FMK for 24 h.

Complex	Ir concentration	Viable	Population (%)		
			Early apoptosis	Late apoptosis	Non-viable
	$0.5 \times IC_{50}$	94.71±0.22	2.61±0.10	2.71±0.22	0.04± 0.02
<b>Ir3 +</b>	$1 \times IC_{50}$	91.32±0.51	6.42±0.11	3.82±2.42	0.08±0.06
<b>Z-VAD-FMK</b>	$2 \times IC_{50}$	91.21±0.41	5.21±0.51	3.62±0.11	0.02±0.01
	$3 \times IC_{50}$	71.43±1.12	14.01±1.52	13.43±0.11	1.21±0.30
<b>Control</b>		96.10±0.08	1.51±0.11	1.32±0.20	0.05±0.03

Table S8. Inhibition of growth of A549 cancer cells by Complex **Ir3** in the presence of different cell death inhibitors recorded over a period of 24 h.

cell death inhibitors	IC <sub>50</sub> (μM) A549
Ir3 + Nec-1	0.30 ± 0.01
Ir3 + 3-MA	4.31 ± 0.02
Ir3 + CHX	1.23 ± 0.05
Ir3 + LPT	0.41 ± 0.04

Table S9. ROS induction in A549 cancer cells treated with complex **Ir3**.

Complex	concentration	ROS (% negative control)
<b>Ir3</b>	$0.25 \times IC_{50}$	6.4±1.0
Untreated cells ( <b>negative control</b> )		1.0 ±0.5
CCCP treated cells ( <b>positive control</b> )		11.5 ±1.8

Table S10. ROS induction in A549 cancer cells treated with cisplatin.

Complex	concentration	ROS (% negative control)
cisplatin	$0.25 \times IC_{50}$	$1.2 \pm 0.8$
Untreated cells <b>(negative control)</b>		$1.0 \pm 0.5$
CCCP treated cells <b>(positive control)</b>		$9.8 \pm 0.9$

Table S11. Cell cycle analysis carried out by flow cytometry using PI staining after exposing A549 cells to cisplatin.

Complex	concentration	Population (%)		
		G <sub>1</sub> phase	S phase	G <sub>2</sub> /M phase
cisplatin	0.25 × IC <sub>50</sub>	8.8±0.6	78.9±3.0	9.9±1.6
	0.5 × IC <sub>50</sub>	6.3±1.0	79.7±1.2	11.3±0.7
	1 × IC <sub>50</sub>	59.1±1.8	33.9±1.0	6.3±0.6
<b>control</b>		49.7±0.4	35.4±1.6	10.7±0.8

Table S12. Cell cycle analysis carried out by flow cytometry using PI staining after exposing A549 cells to complex **Ir3**.

Complex	Ir concentration	Population (%)		
		G <sub>1</sub> phase	S phase	G <sub>2</sub> /M phase
<b>Ir3</b>	0.25 × IC <sub>50</sub>	62.8±0.2	27.8±2.9	5.5±0.3
	0.5 × IC <sub>50</sub>	66.8±0.1	25.7±1.6	6.5±0.1
	1 × IC <sub>50</sub>	70.1±1.2	26.6±0.4	9.0±1.2
<b>control</b>		57.0±2.5	30.8±1.7	7.9±0.9

Table S13. Effects of **Ir3** on MMP analyzed by JC-1 staining and flow cytometry. A549 cells were treated with vehicle or metal at the indicated concentrations for 24 h.

Complex	Concentration	Population (%)	
		JC-1 Aggregates	JC-1 Monomers
<b>Ir3</b>	0.25 × IC <sub>50</sub>	88.2±0.8	11.7±0.8
	0.5 × IC <sub>50</sub>	78.9±3.2	21.0±3.2
	IC <sub>50</sub>	72.3±0.4	26.3±1.1
	2 × IC <sub>50</sub>	58.2±0.9	41.8±0.8
<b>Negative Control</b>		89.3±0.3	10.6±0.3
<b>Positive Control</b>		18.6±0.5	81.3±0.5

Table S14. Effects of cisplatin on MMP analyzed by JC-1 staining and flow cytometry. A549 cells were treated with vehicle or cisplatin at the indicated concentrations for 48 h.

Complex	Concentration	Population (%)	
		JC-1 Aggregates	JC-1 Monomers
cisplatin	0.25 × IC <sub>50</sub>	92.4±0.5	7.6±1.2
	0.5 × IC <sub>50</sub>	91.9±2.4	8.1±1.1
	IC <sub>50</sub>	3.5±0.2	96.5±3.2
	2× IC <sub>50</sub>	1.5±0.2	98.5±2.8
<b>Negative Control</b>		92.8±1.6	7.2±0.5
<b>Positive Control</b>		10.2±0.9	89.9±1.4

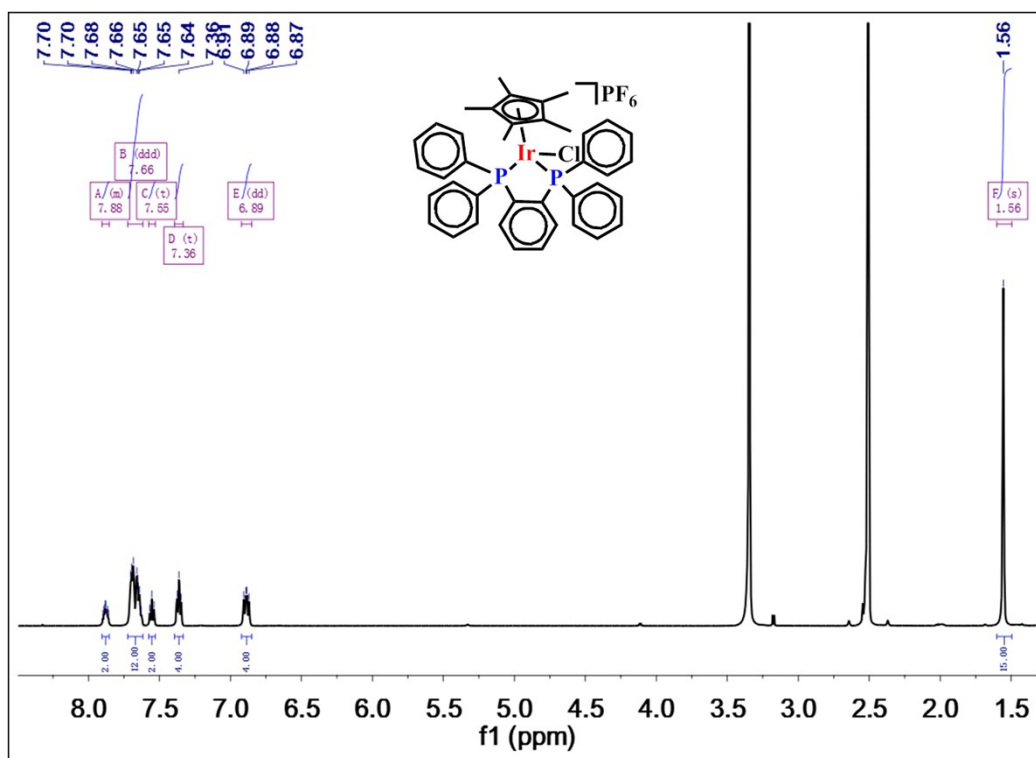


Fig. S9. The  $^1\text{H}$  NMR (500 MHz, DMSO) peak integrals of complex  $[(\eta^5\text{-Cp}^*)\text{Ir}(\text{L1})\text{Cl}]\text{PF}_6$  (**Ir1**).

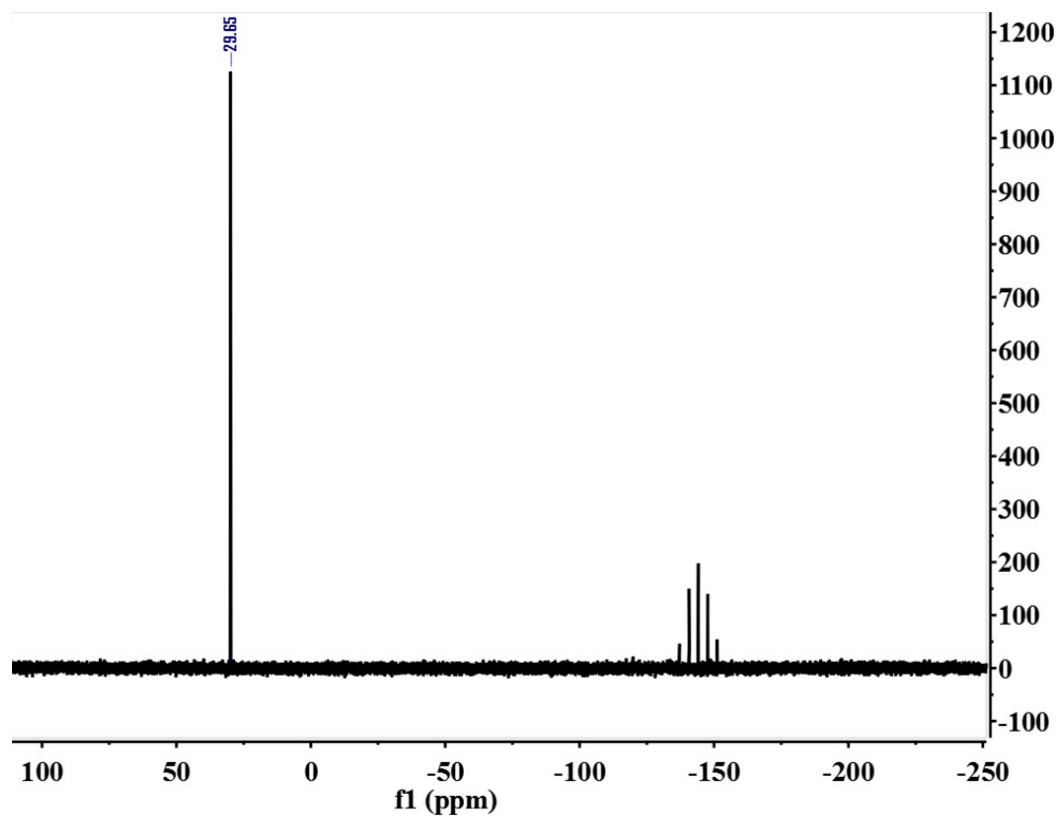


Fig. S10. The  $^{31}\text{P}$  NMR (500 MHz, DMSO) peak integrals of complex  $[(\eta^5\text{-Cp}^*)\text{Ir}(\text{L1})\text{Cl}]\text{PF}_6$  (**Ir1**).

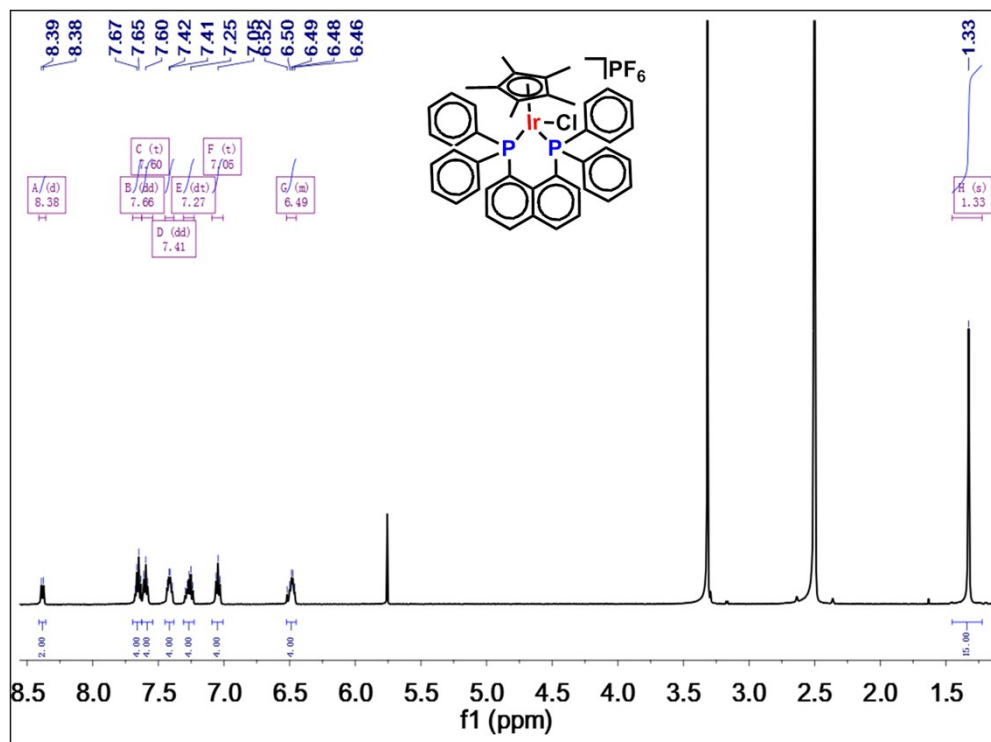


Fig. S11. The  $^1\text{H}$  NMR (500 MHz, DMSO) peak integrals of complex  $[(\eta^5\text{-Cp}^*)\text{Ir}(\text{L}2)\text{Cl}]\text{PF}_6$  (**Ir2**)

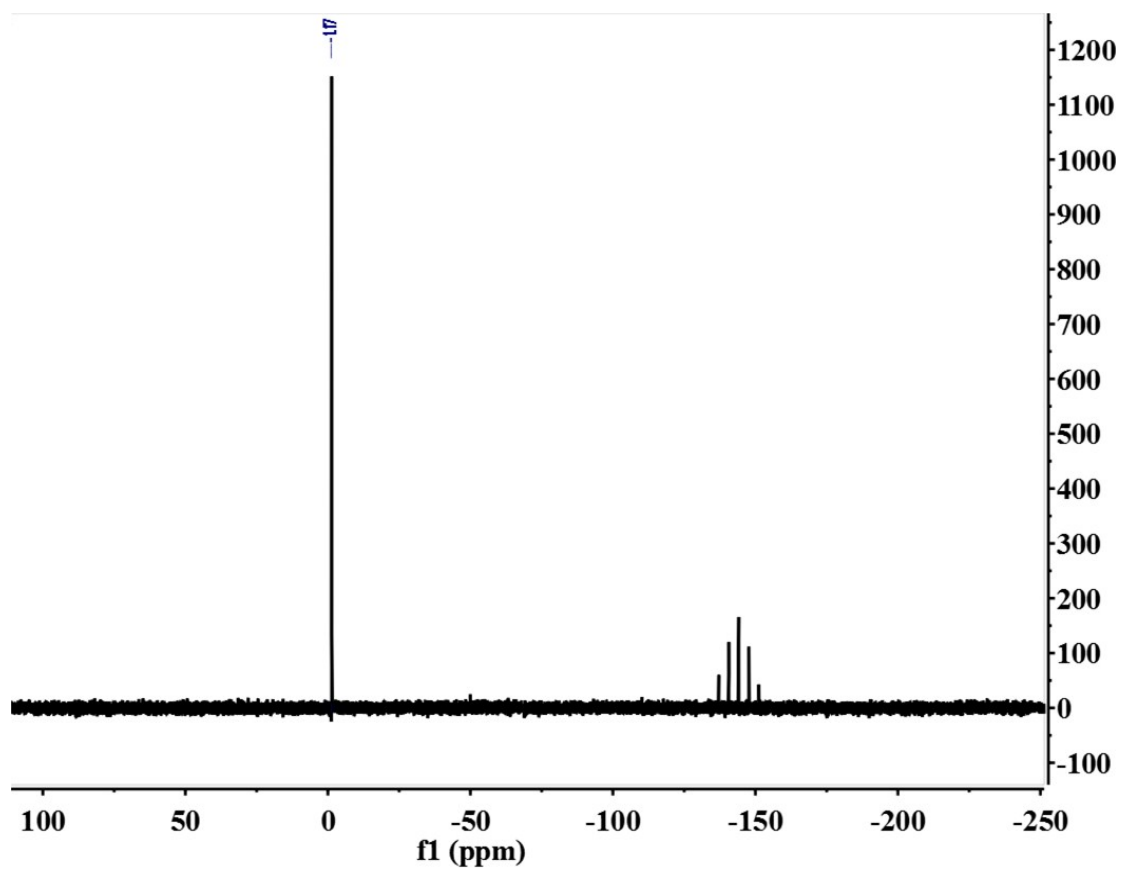


Fig. S12. The  $^{31}\text{P}$  NMR (500 MHz, DMSO) peak integrals of complex  $[(\eta^5\text{-Cp}^*)\text{Ir}(\text{L}2)\text{Cl}]\text{PF}_6$  (**Ir2**).

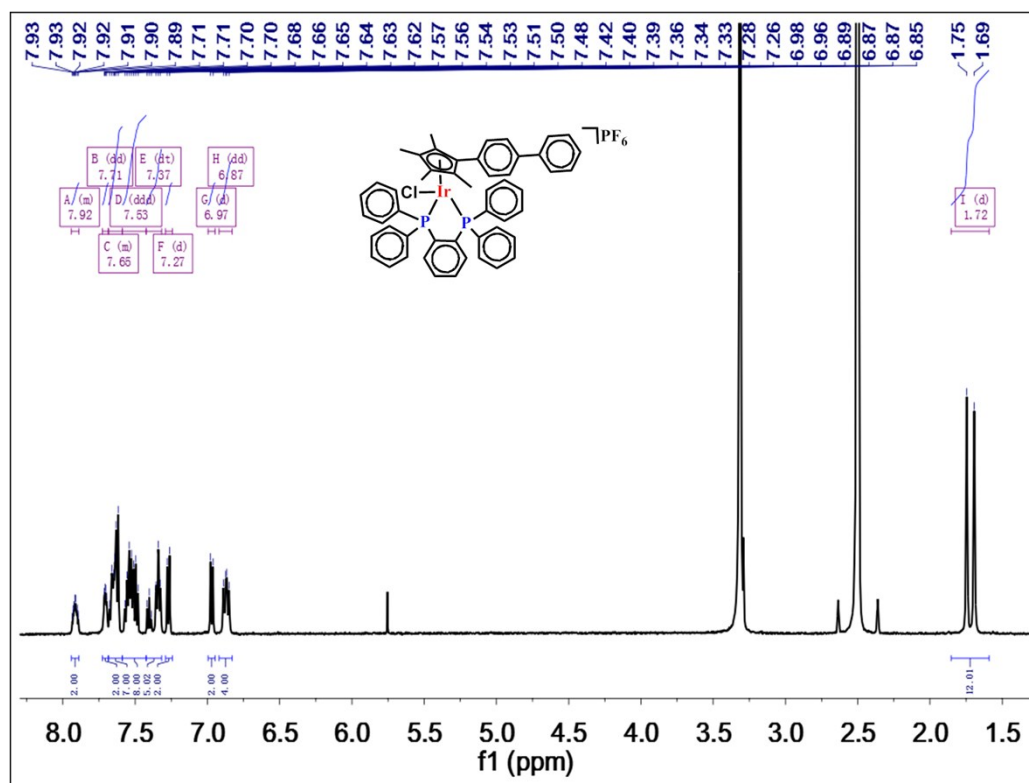


Fig. S13. The  $^1\text{H}$  NMR (500 MHz, DMSO) peak integrals of complex  $[(\eta^5\text{-Cp}^{\text{xbiph}})\text{Ir}(\text{L1})\text{Cl}]\text{PF}_6$  (**Ir3**)

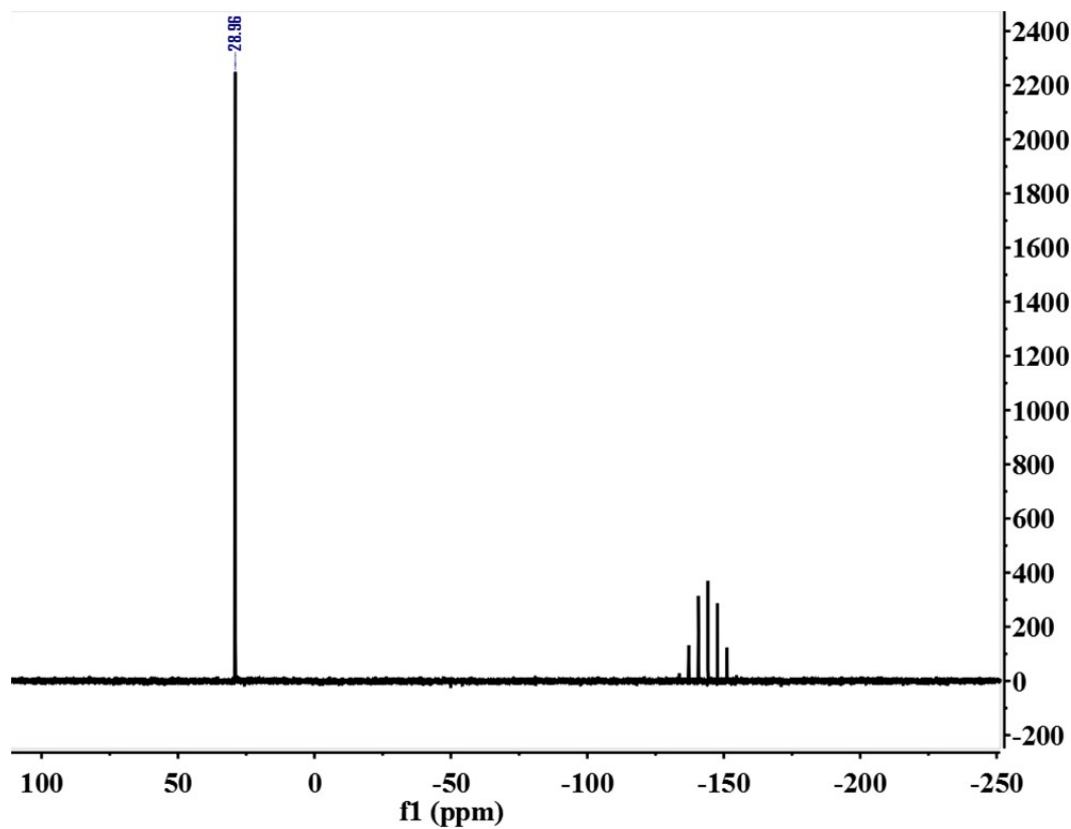


Fig. S14. The  $^{31}\text{P}$  NMR (500 MHz, DMSO) peak integrals of complex  $[(\eta^5\text{-Cp}^{\text{xbiph}})\text{Ir}(\text{L1})\text{Cl}]\text{PF}_6$  (**Ir3**)

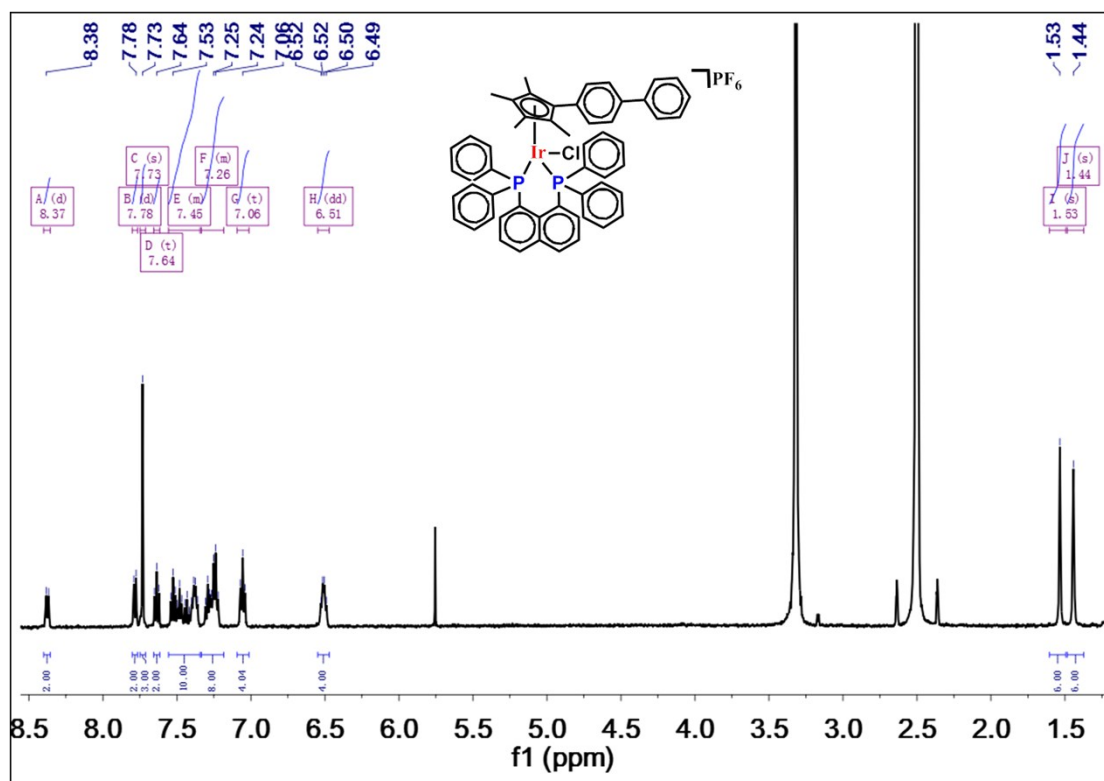


Fig. S15. The  $^1\text{H}$  NMR (500 MHz, DMSO) peak integrals of complex  $[(\eta^5\text{-Cp}^{\text{xbiph}})\text{Ir}(\text{L2})\text{Cl}]\text{PF}_6$  (**Ir4**).

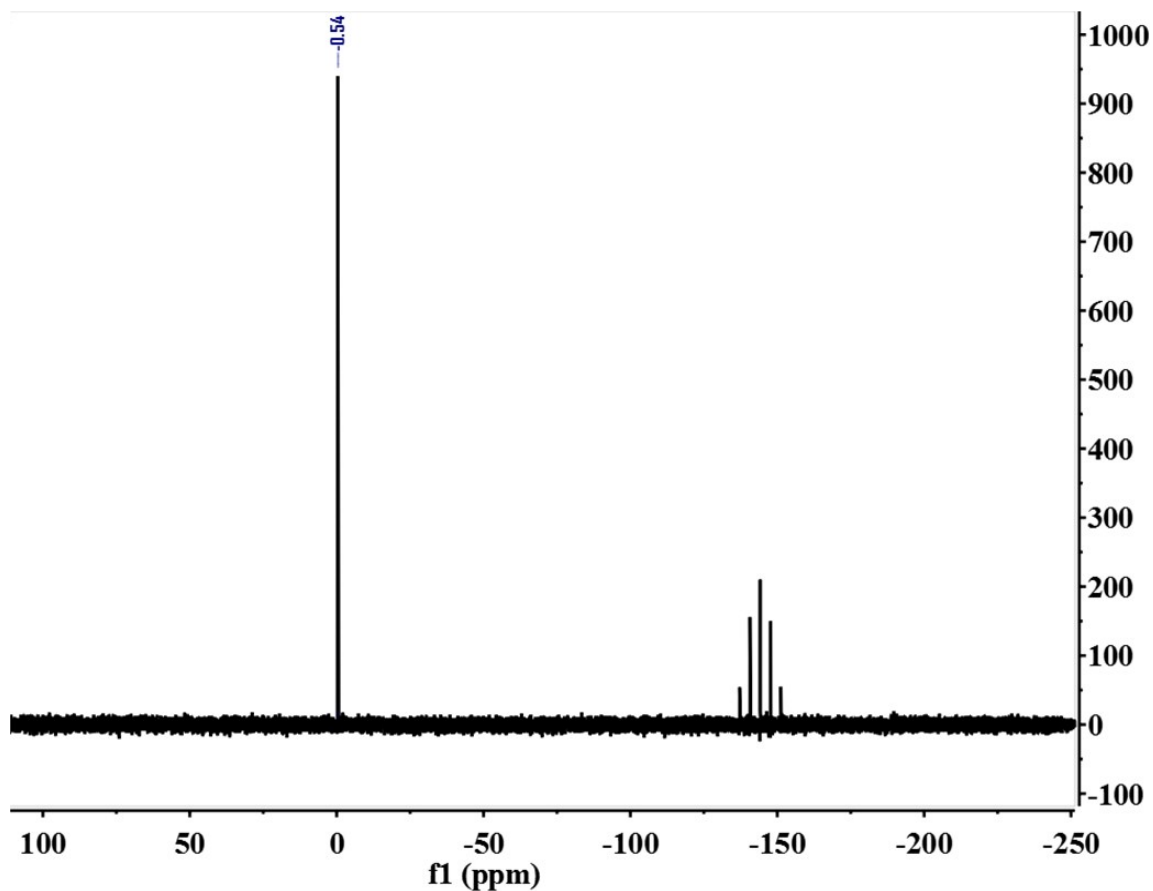


Fig. S16. The  $^{31}\text{P}$  NMR (500 MHz, DMSO) peak integrals of complex  $[(\eta^5\text{-Cp}^{\text{xbiph}})\text{Ir}(\text{L2})\text{Cl}]\text{PF}_6$  (**Ir4**).

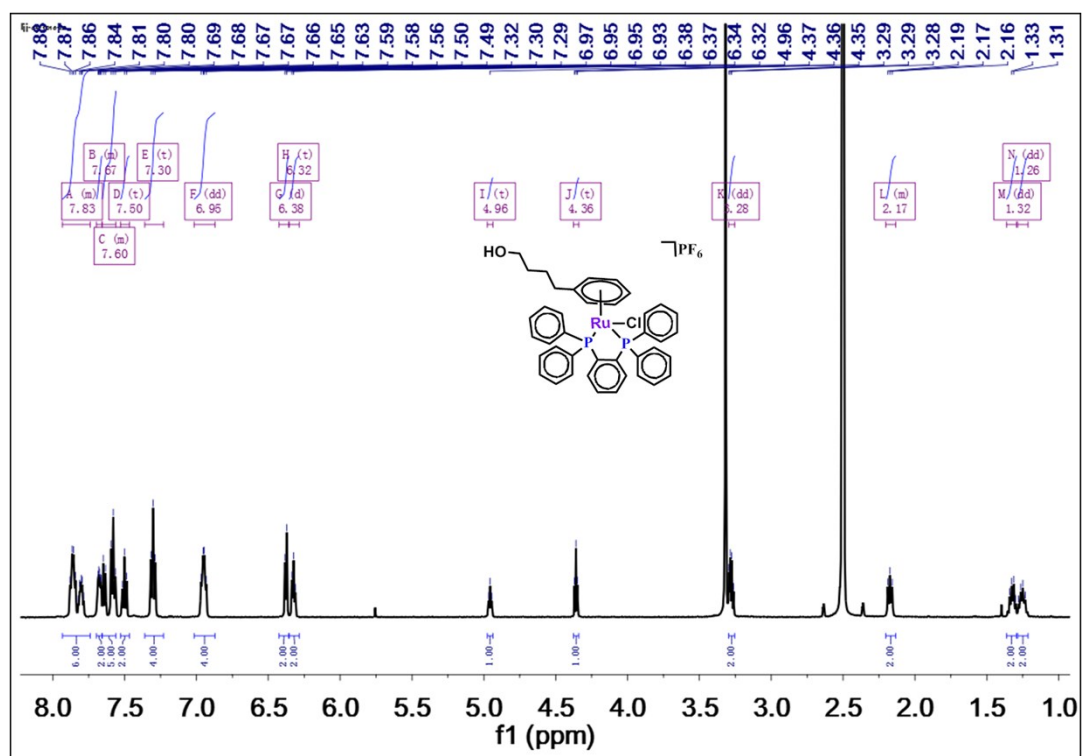


Fig. S17. The  $^1\text{H}$  NMR (500 MHz, DMSO) peak integrals of complex  $[(\eta^6\text{-bz-BA})\text{Ru}(\text{L1})\text{Cl}]\text{PF}_6$  (**Ru1**).

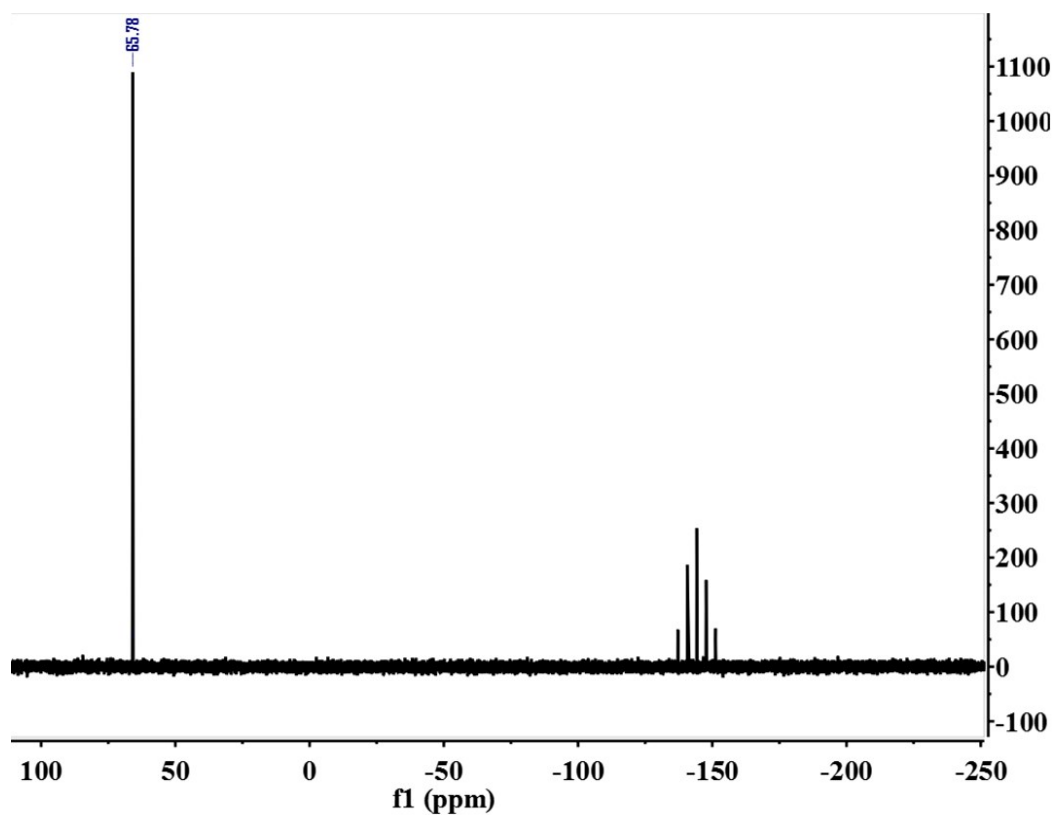


Fig. S18. The  $^{31}\text{P}$  NMR (500 MHz, DMSO) peak integrals of complex  $[(\eta^6\text{-bz-BA})\text{Ru}(\text{L1})\text{Cl}]\text{PF}_6$  (**Ru1**).

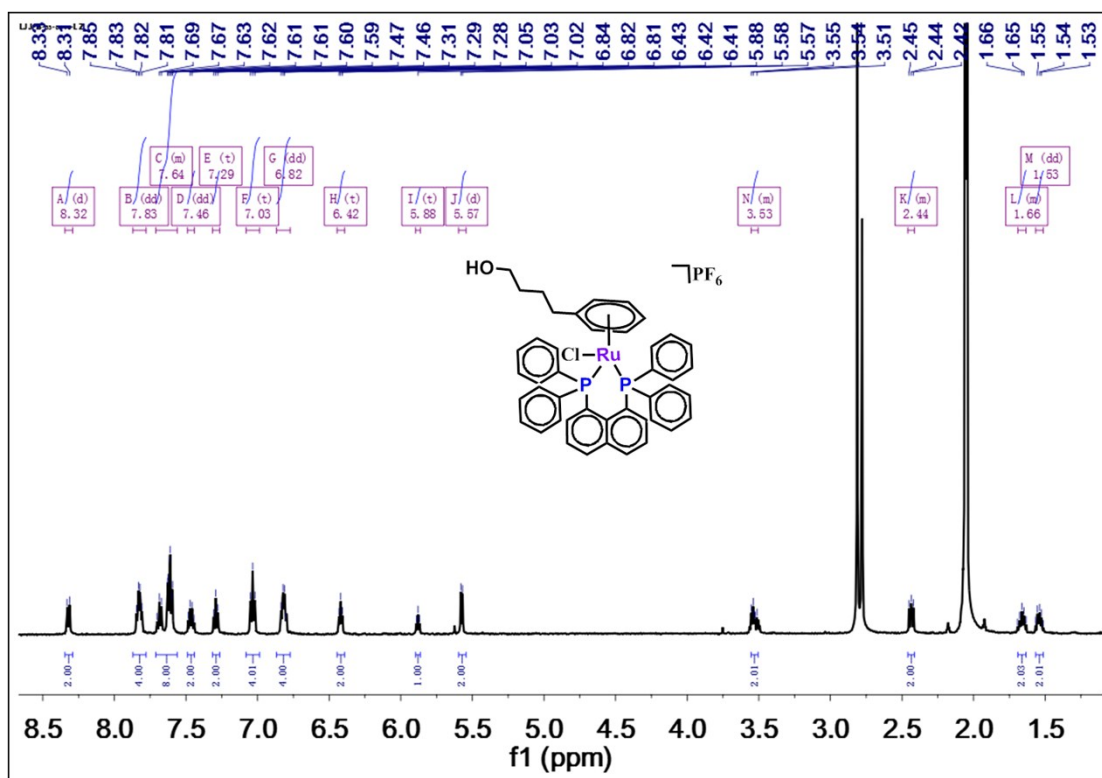


Fig. S19. The  $^1\text{H}$  NMR (500 MHz, Acetone) peak integrals of complex  $[(\eta^6\text{-bz-BA})\text{Ru}(\text{L}2)\text{Cl}]\text{PF}_6$  (**Ru2**).

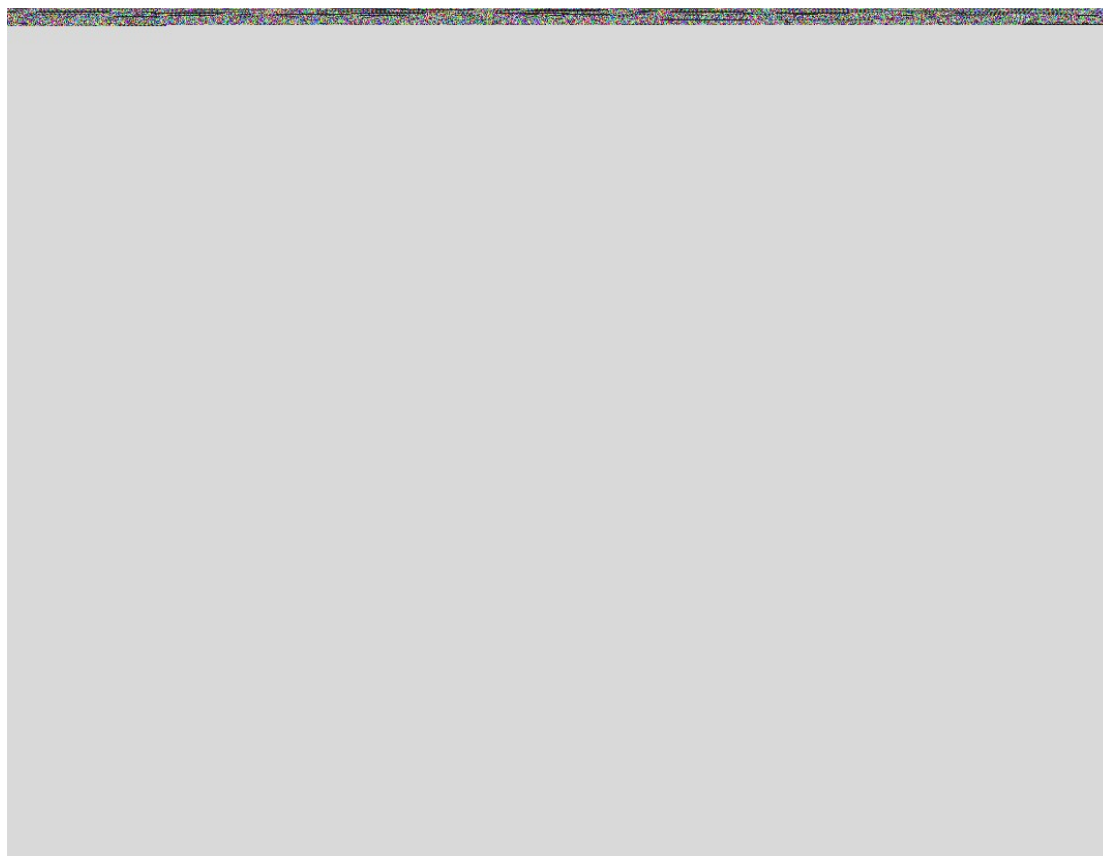


Fig. S20. The  $^{31}\text{P}$  NMR (500 MHz, Acetone) peak integrals of complex  $[(\eta^6\text{-bz-BA})\text{Ru}(\text{L}2)\text{Cl}]\text{PF}_6$  (**Ru2**).

#### References.

1. Wang, C.; Liu, J.; Tian, Z.; Tian, M.; Tian, L.; Zhao, W.; Liu, Z. Half-sandwich iridium N-heterocyclic carbene anticancer complexes. *Dalton Trans.* **2017**, 46, 6870-6883.
2. Li, J.; Tian, M.; Tian, Z.; Zhang, S.; Yan, C.; Shao, C.; Liu, Z. Half-Sandwich Iridium(III) and Ruthenium(II) Complexes Containing P<sup>^</sup>P-Chelating Ligands: A New Class of Potent Anticancer Agents with Unusual Redox Features. *Inorg. Chem.* **2018**, 57, 1705-1716.